JOURNAL OF CATALYSIS 100, 446–457 (1986)

The Microstructure of Bimetallic Ru–Cu/SiO_2 Catalysts: A Chemisorption and Analytical Electron Microscopy Study

A. G. SHASTRI, J. SCHWANK,[1] AND S. GALVAGNO*

*Department of Chemical Engineering, The University of Michigan, Ann Arbor, Michigan 48109-2136; and *Istituto CNR-TAE, Via S. Lucia, 39, Pistunina-Messina, Italy*

Received December 11, 1985; revised April 1, 1986

Supported bimetallic Ru–Cu/SiO_2 catalysts are characterized by transmission electron microscopy, energy dispersive X-ray spectroscopy, electron microdiffraction, and chemisorption. Metal particles up to 4 nm in diameter are bimetallic, while particles larger than 4 nm contain only Cu. Considerable compositional nonuniformity is observed from one individual metal particle to the next. Microdiffraction patterns obtained from individual particles can be attributed to either Ru or Cu suggesting no significant modification in crystallographic structure of either metal component. Addition of Cu to Ru results in a drastic suppression of H_2 chemisorption while the extent of O_2 chemisorption is not as strongly affected. The suppressed H_2 chemisorption capability of Ru in the bimetallic catalysts is an indication of atomic interdispersion of Ru and Cu on the surface of the bimetallic clusters, leading to the break-up of the Ru ensembles which would be necessary for dissociation of molecular hydrogen. The influence of catalyst preparation techniques on the relative interdispersion of Ru and Cu and consequent discrepancies in the Ru–Cu literature are discussed.

INTRODUCTION

Supported bimetallic Ru–Cu catalysts (*1–9*) and single crystal Ru surfaces covered by Cu (*10–15*) have been the subjects of extensive research. Conflicting results have been reported on the influence of Cu on H_2 chemisorption. On SiO_2 supported Ru–Cu catalysts, Sinfelt *et al.* (*1–3*) reported a Cu-induced suppression of H_2 chemisorption while Haller and co-workers (*8, 9*) did not find any significant influence of Cu on the H_2 chemisorption capability of Ru. On Cu-covered Ru(0001) surfaces, a suppression of H_2 adsorption capacity was found by Ertl and co-workers (*10, 11*), in contrast to Goodman *et al.* (*15*) who reported that Cu attenuated the H_2 chemisorption on ruthenium via a simple site blocking mechanism. Differences in opinion also exist concerning the effect of copper on the ethane hydrogenolysis activity of ruthenium. Both Sinfelt (*2*) and Haller (*8, 9*) found on supported catalysts a significant reduction in the catalytic activity of Ru with the addition of Cu. Recent work by Peden and Goodman (*14*) on single crystals shows no significant change in hydrogenolysis activity (normalized with respect to ruthenium surface sites) as a function of Cu content. A similar discrepancy is also seen in the case of CO hydrogenation on Ru–Cu/SiO_2 catalysts. Lai and Vickerman (*7*) reported that the activity for CO disproportionation and CO hydrogenation were drastically reduced by the presence of Cu. King *et al.* (*37*), on the other hand, reported that the decrease in the rate of CO hydrogenation was proportional to the decrease in the amount of Ru on the catalyst surface. While hydrogen spillover from Ru to Cu was not observed at 150 K (*11, 12*), spillover may become significant at 230 K. Temperature-programmed desorption cannot discriminate between hydrogen bonded to Ru vs hydrogen bonded to Cu (*16*). Hydrogen spillover could, according to Goodman (*16*), result in a possible overcount of Ru sites, leading to erroneously low turnover frequencies. However, Sinfelt (*2*) and

[1] To whom all correspondence should be addressed.

0021-9517/86 $3.00

Haller (*8, 9*) have reported their activities normalized with respect to adsorbed hydrogen. Thus the activities reported by Sinfelt and Haller represent a conservative estimate even if spillover from Ru to Cu should have contributed to enhanced H_2 uptake.

One can reconcile the different observations by these various research groups, if the catalyst preparation procedures are examined in careful detail. Sinfelt (*1*) used $RuCl_3$ and $Cu(NO_3)_2$ precursor salt solutions for coimpregnation of Cab-O-Sil HS5 silica support (S.A. 300 m^2/g) in contrast to $Ru(NO)(NO_3)_2 \cdot H_2O$ and $Cu(NO_3)_2 \cdot 6H_2O$ used by Haller (*8, 9*) for the impregnation of Davison silica (S.A. 600 m^2/g). The anion of the impregnating solution and the porous structure of the support can have a significant influence on the Ru dispersion and on the formation of Ru–Cu bimetallic clusters (*9*). Previous work in this laboratory dealing with supported bimetallic Ru–Au catalysts has shown that the nature of the support, the details of catalyst preparation, and the reduction medium (H_2 vs N_2H_4) can have a dramatic influence on bimetallic cluster formation, metal dispersion, and consequently catalytic activities (*17–26*). Similarly, the conflicting results in single crystal studies (*10–16*) may very well be due to differences in the substrate temperature used during Cu deposition [540 or 180 K used by Ertl (*10*) versus 100 K used by Goodman (*15*)]. Ertl *et al.* (*10*) have reported the formation of three-dimensional Cu islands at 540 K, while two-dimensional Cu growth phases on Ru(0001) surfaces are formed at 1080 K. Cu island formation on Ru(0001) at 500 K is predicted by a recent Monte Carlo simulation (*37*). The above discussion has clearly shown a need for more research work to enhance our understanding of Group VIII–Group Ib bimetallic systems, in particular the role of preparative variables on the formation of bimetallic clusters. Previously, a multifaceted characterization approach (*19*) was applied to the Ru–Au bimetallic system in order to correlate the structure and morphology of these catalysts with activity and selectivity trends for ethane hydrogenolysis (*22*) and CO hydrogenation (*17, 18*). Our objective here was to apply a similar multifaceted characterization approach to supported Ru–Cu catalysts, with special emphasis on analytical electron microscopy and chemisorption/surface titration techniques. A transmission electron microscopy study of supported Ru–Cu catalysts has been reported previously where the predominant morphology of the metal particles was in the form of thin, raft-like structures (*4*). In a previous analytical electron microscopy study of Ru–Cu/SiO_2 catalysts (*7*) no unambiguous information on the existence and characteristics of bimetallic Ru–Cu particles could be derived, as the study was carried out on Cu grids precluding the detection of Cu in the catalyst metal particles.

To the best of our knowledge, no other analytical electron microscopy study of the supported Ru–Cu system has been published. We have combined bright field transmission imaging (TEM), energy dispersive X-ray spectroscopy (EDS), and microdiffraction to derive morphological, analytical, and structural information from individual metal particles in the supported Ru–Cu/SiO_2 catalysts. The following questions are of specific interest: are the individual particles in our Ru–Cu catalysts bimetallic or monometallic? What particle-size range is the most dominant one in terms of contribution to the metal surface area? Is there a particular size range favoring the formation of bimetallic clusters? Can chemisorption and H_2/O_2 titration be used for determining the dispersion of the two metal components in the Ru/Cu system?

EXPERIMENTAL

The Ru–Cu/SiO_2 catalysts were prepared by coimpregnating Davison 951 N SiO_2 with aqueous solutions of $RuCl_3 \cdot H_2O$ (Rudi Pont, Reagent Grade) and $Cu(NO_3)_2 \cdot 3H_2O$ (Baker Analyzed Reagent). The SiO_2

TABLE 1

Chemisorption Data on Bimetallic Ru–Cu/SiO_2 Series

Sample code[a]	Metal content (wt%)		H_2 uptake at 298 K			H_{rev}/H_{total} (298 K)	O_2 uptake at 298 K			O_2 molecules/ total metal atoms	O_2 uptake/ H_2 uptake
	Ru	Cu	cm^3(STP)/g	% D	d^b (nm)		cm^3(STP)/g	% D	d^c (nm)		
RCS100	2.1	—	0.85	36.5	2.5	—	1.72	36.9	2.48	0.369	2.02
RCS034	1.2	1.45	0.105	7.9	115.8	0.16	1.09			0.141	10.4
RCS008	0.3	2.10	0.024	7.2	126.7	0.29	0.465			0.058	19.4
RCS000	—	1.9	0	—	—	—	0.096	5.7	18.2	0.014	—

[a] The three-digit number represents the atomic percentage of Ru with respect to total metal content.
[b] Assuming monometallic Ru particles and Ru–H stoichiometry.
[c] Assuming RuO_2 stoichiometry and Cu_2O stoichiometry.

support as supplied from the manufacturer had a BET surface area of 650 m^2/g. The impregnated samples were dried for 4 h at 383 K, followed by H_2 reduction for 20 h at 673 K. The reduced catalysts had BET surface areas of 565 ± 22 m^2/g. Table 1 summarizes the metal loadings for the various catalysts.

The chemisorption experiments were carried out in a static volumetric Pyrex glass high-vacuum system. Research grade gases were used for catalyst pretreatment and chemisorption. Prior to chemisorption, the prereduced catalysts were treated in hydrogen at 400°C for 20 h followed by evacuation. The amount of strongly bound gas was measured by taking the difference between two isotherms obtained sequentially. The first isotherm provided information about the total gas uptake. The second isotherm, taken after 30 min evacuation, gave the amount of weakly adsorbed H_2. Typical equilibration times were 12 h for the first adsorption point and 1 h for subsequent adsorption points. Average metal particle sizes were calculated by using the equation $d = 6/s\rho$, where s = metal surface area/g of metal, ρ = density of metal. Cross-sectional areas of 9.03 A^2 per Ru atom (*24*) and 6.8 A^2 per Cu atom (*35*) were assumed.

The total surface areas of the catalysts were determined by the single-point BET technique in a Quantachrome Monosorb Surface Area Analyzer with N_2 at 77.3 K as adsorbate. X-Ray diffraction studies were carried out in a Philips X-ray diffractometer with monochromatic Cu$K\alpha$ as the radiation source. Metal crystallite sizes were obtained from X-ray line broadening using Scherrer's equation after correcting for the instrumental contribution.

Electron microscopy studies were carried out in a JEOL-100CX microscope equipped with a side-entry goniometer stage, and ASID-4D scanning attachment and a lithium-drifted solid-state X-ray detector for elemental analysis. Data acquisition was carried out with a multichannel analyzer connected to a ND6620 computer. Microscopy specimen were prepared by placing the catalyst powder on holey carbon film mounted on a Be grid. Metal particle size distributions were obtained by counting several hundred particles in the high-resolution transmission electron microscopy images. Three statistical averages, namely the number average d_n, surface average d_s, and volumetric average particle size d_v were calculated using the equations

$$d_n = \frac{\sum n_i d_i}{\sum n_i},$$

$$d_s = \frac{\sum n_i d_i^3}{\sum n_i d_i^2},$$

$$d_v = \frac{\sum n_i d_i^4}{\sum n_i d_i^3},$$

where n_i represents the number of metal particles of size d_i (nm). For elemental analysis of individual metal particles, a suitable sampling area was identified and photographed in the transmission mode and then the microscope was switched over to the scanning transmission mode for energy dispersive spectroscopy. A 10-nm electron probe was focused on individual metal particles of interest and X-ray counts were acquired for 200 s. The JEOL-100CX machine has been suitably modified by employing Pt augmented apertures for the condenser lens, proper detector geometry, and a hard X-ray aperture to eliminate spurious X-rays generated within the column (*28*). A zero "hole-count" through the holes of holey carbon-covered Be grids was ensured for microanalysis. Beam broadening can be estimated by using the single scattering equation proposed by Goldstein *et al.* (*29*).

$$B = 625 \cdot \left(\frac{\rho}{A}\right)^{0.5} \cdot \frac{Z}{E} \cdot t^{1.5}$$

where B = beam broadening in cm, ρ is density in g/cm^3, A is atomic weight, Z is atomic number, E is accelerating voltage of the microscope in kV, and t is the sample thickness in cm. For a 100-nm-thick SiO_2 sample, B amounts to 3.8 nm. By ensuring that no other metal particle is within 10 nm of the analyzed metal particle, X-ray signals from individual small metal particles can be obtained. To further confirm that beam broadening is not causing artifacts in the EDS spectra, the beam was moved away from an analyzed metal particle to an adjacent, metal-free region, and only Si signals were seen. Further precautions were taken by using a carbon boat and a custom-built aluminum sample holder to eliminate artifacts in the EDS spectra. However, the low X-ray count and the poor signal-to-noise ratio does not allow any quantification of the EDS results generated from such small metal particles. For obtaining microdiffraction patterns, a sharp image of a suitable specimen area was first obtained in the scanning transmission mode (STEM). A condenser aperture of 20 μm and a 10-nm probe size were used to obtain electron microdiffraction patterns. A thin polycrystalline Au film standard was used to calibrate the camera length for specific values of condenser and intermediate lens current and specimen position.

RESULTS AND DISCUSSION

Chemisorption Studies

Table 1 summarizes the pertinent chemisorption data for the Ru–Cu/SiO_2 catalysts. Addition of Cu results in suppression of H_2 chemisorption, in agreement with the observations of Sinfelt (*1–3*) and Ertl (*10, 11*). It has been suggested that a minimum of six adjacent Ru surface sites is required for H_2 dissociation (*11, 13*). It appears that Cu, when properly dispersed on the Ru surface, can disrupt the Ru ensembles required for H_2 dissociation. This would result in a decrease in the amount of dissociatively adsorbed hydrogen. Interestingly, no such evidence for a disruption of ensembles needed for H_2 dissociation was found in the Ru–Au/SiO_2 system (*17, 23*) despite the fact that both Ru and Au were located within small metal particles of <4 nm in diameter. The discrepancy between Ru–Cu/SiO_2 and Ru–Au/SiO_2 may be due to differences in the interdispersion of the two metal components within the bimetallic "clusters." Similar observations have been made by Haller and co-workers on Ru–Cu/SiO_2 and Ru–Ag/SiO_2 catalysts: Cu tends to form two-dimensional rafts on the Ru surface whereas Ag exists in the form of three-dimensional islands (*8*).

The amount of reversibly adsorbed hydrogen which can be evacuated at 298 K (expressed as percentage of total H_2 uptake) increases as a function of Cu content. Such a reversible hydrogen adsorption may arise from a combination of physical adsorption and/or weak chemisorption. In the case of monometallic Ru, the reversibility of hydrogen adsorption seems to be a function of the metal dispersion (*23–25, 36*).

Depending on the metal particle size distribution of a given catalyst, the ratio of surface sites which are responsible for strong vs weak chemisorption of hydrogen may change. Adding Cu to Ru is likely to cause a modification of the Ru surface site distribution and Ru ensemble size. In the case of our Ru–Cu/SiO_2 catalysts where the two metal components are intimately interdispersed within small metal particles, Cu seems to increase the relative concentration of Ru sites for weak H_2 chemisorption at the expense of Ru sites for strong H_2 chemisorption. This effect of Cu on the reversibility of hydrogen adsorption could simply be a manifestation of the geometric disruption of Ru ensembles. However, some electronic interaction between Ru and Cu could also contribute to the modification of the adsorption properties of Ru. It should be noted that in the case of small bimetallic Ru–Au particles the extent of reversible hydrogen adsorption slightly decreased with increasing Au content (*23*). We suspect that these differences are due to differences in the interdispersion of the metal components on the surface of the small particles.

Another complication that needs to be taken into account is the possibility of hydrogen spillover from Ru to Cu sites. Goodman and Peden (*16*) reported that it is not possible to distinguish on the basis of temperature-programmed desorption between atomic hydrogen adsorbed on Ru or Cu sites. Hydrogen spillover should lead to an increase in hydrogen uptake beyond the amount of hydrogen that can be accommodated on Ru surface sites. The fact that we do not observe such an increase in hydrogen uptake as Cu is added to Ru indicates that in our catalysts Cu inhibits the dissociation of molecular hydrogen on Ru. The dissociation of molecular hydrogen would be a prerequisite for spillover of atomic hydrogen from Ru to Cu sites.

Judging from the literature, the extent of disruption of Ru ensembles by Cu can vastly differ depending on the catalyst preparation conditions. Consequently, there are cases where one observes increased hydrogen uptake due to spillover from Ru to Cu sites (*16*) while in other instances a decrease of H_2 uptake is reported (*1–3, 10–12*). The data reported here fall into the category of decreased H_2 chemisorption with a negligible contribution of spillover due to insufficient hydrogen dissociation. H_2 adsorption may not in all cases be suitable for measuring the Ru dispersion and for normalizing the turnover frequencies for bimetallic Ru–Cu catalysts. Depending on whether the ensemble effect leading to decreased H_2 uptake or the spillover of H_2 leading to increased H_2 uptake is dominant, turnover frequencies normalized with respect to chemisorbed hydrogen can either be too large or too small.

In view of the difficulties associated with H_2 adsorption, O_2 was brought in as a second adsorbate. On the monometallic Cu/SiO_2 catalyst RCS000, a small amount of O_2 (0.096 cm^3(STP)/g) was adsorbed at 298 K. The formation of Cu_2O upon dissociation of molecular O_2 has been reported in an EELS study at temperatures between 298 and 523 K (*30*). Previous IR (*31*), electron diffraction (*32*), and X-ray diffraction (*33*) studies have also indicated the formation of Cu_2O. The formation of CuO requires temperatures much higher than 523 K. We cannot be sure that the O_2 adsorption at 298 K led to complete monolayer coverage on Cu/SiO_2. However, an assumption of a Cu_2O adsorption stoichiometry leads to an average Cu particle size of 18.2 nm, in good agreement with the average Cu particle size determined from X-ray diffraction (22.4 nm). The oxygen adsorbed on the Cu/SiO_2 catalyst did not show any measurable reactivity toward H_2 at 298 K. Increasing the O_2 adsorption temperature to 373 K led to a significant increase in O_2 uptake from 0.096 to 1.46 cm^3(STP)/g indicating a reaction of subsurface Cu with oxygen. At 373 K, there was significant activity in the H_2/O_2 titration leading to a H_2 consumption of 2.456 cm^3(STP)/g.

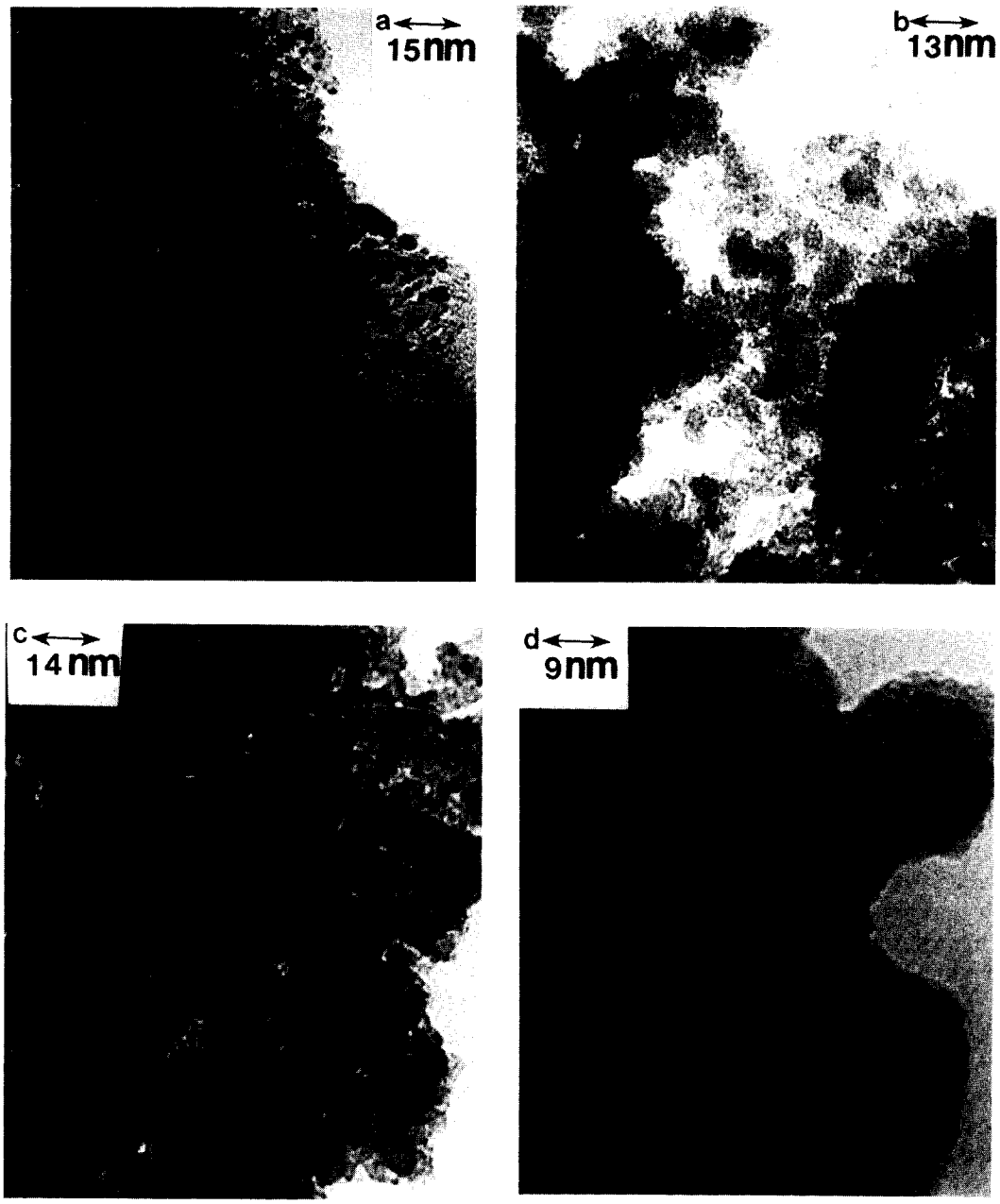

FIG. 1. Representative bright-field transmission electron micrographs. (a) Catalyst RCS000, (b) catalyst RCS034, (c) catalyst RCS008, (d) catalyst RCS100.

In bimetallic Ru–Cu catalysts, oxygen adsorption takes place on both Ru and Cu sites at a temperature of 298 K. However, the adsorption stoichiometries are different, corresponding to RuO_2 and Cu_2O, respectively. Experiments with physical mixtures of the monometallic catalysts RCS100 and RCS000 proved that the oxygen uptake at 298 K can be explained as a linear combination of the uptakes expected for the two

individual metal components. In the bimetallic Ru–Cu/SiO_2 catalysts, the oxygen uptake expressed per metal atom in the catalyst decreases as the Cu content increases (Table 1). Since, due to the adsorption stoichiometry, 4 Cu atoms are required to accommodate one O_2 molecule vs 1 Ru atom per O_2 molecule, the decrease in O_2 uptake indicates the presence of finely dispersed Cu on the Ru surface. It is, however, difficult to discern whether there is a similar linear combination of O_2 uptake on Ru and Cu sites at work, or whether there is a change in the adsorption behavior of either metal component in the bimetallic clusters. In EXAFS studies of Ru and Ru–Cu clusters, Sinfelt *et al.* (*27*) reported that on monometallic Ru, O_2 molecules are adsorbed in an "end-on" configuration at positions of threefold symmetry in relation to the ruthenium surface atoms. The presence of Cu tends to shield the Ru from oxygen. According to Shi *et al.* (*34*), Cu reduces the initial sticking coefficient of O_2 for clean Ru surfaces by a simple site blocking mechanism, while it significantly retards the initial dissociative chemisorption of N_2O. A fairly large ensemble of up to 18 Ru surface atoms seems to be necessary for the N_2O dissociation to proceed, and the characteristics of chemisorbed oxygen on Cu seem to be modified by the presence of Ru.

Since neither H_2, O_2, nor N_2O adsorption seem to provide an unambiguous measure of Ru and Cu surface sites, H_2/O_2 titration experiments were attempted. The titration reaction appears in principle promising for discerning between Ru and Cu sites. In a similar bimetallic system, namely Ru–Au, the H_2/O_2 titration at 373 K was successfully used for an independent determination of the Ru and Au dispersion (*23*). At 373 K, only the oxygen adsorbed on Ru sites was titratable, while oxygen on Au sites had negligible reactivity toward H_2. Unfortunately, in the Ru–Cu system the titration temperature of 373 K is unsuitable as Cu by itself has a significant titration activity at this temperature. The undesirable titration activity of Cu can be reduced to a negligible level by lowering the temperature to 298 K. However, at this temperature very long equilibration times become necessary even for the reaction on Ru sites, making the procedure impractical.

Electron Microscopy Studies

In order to understand whether the metal components are indeed bimetallic clusters, a careful characterization by analytical electron microscopy was carried out.

Several transmission electron micrographs for each catalyst were taken in order to derive reliable statistical averages for particle size distributions. Figure 1 shows representative micrographs. Figure 2 represents the particle size histograms for the bimetallic samples. The number average, d_n, surface average, d_s, and volume average particle size, d_v, obtained from microscopy are summarized in Table 2. For one sample of catalyst RCS034, average particle sizes were obtained before and after an additional treatment in H_2 at 400°C for 24 h in order to check the thermal stability of the particle size distribution. No significant change was observed after the above thermal treatment as can be seen from Table 2. The hydrogen uptake on the bimetallic catalysts is so severely suppressed that average particle sizes calculated from chemisorption (Table 1) are completely out of range compared to the size of metal particles actually observed by electron microscopy (Table 2). This massive discrepancy

TABLE 2

TEM Particle Size Data on Ru–Cu/SiO_2 Series

Sample code	d_n (nm)	d_s (nm)	d_v (nm)
RCS100	1.66	1.82	1.87
RCS034	1.7	2.2	2.44
RCS034[a]	1.95	2.49	2.79
RCS008	3.1	4.1	4.5
RCS000	10.25	12.11	16.58

[a] After additional 24 h H_2 reduction at 400°C.

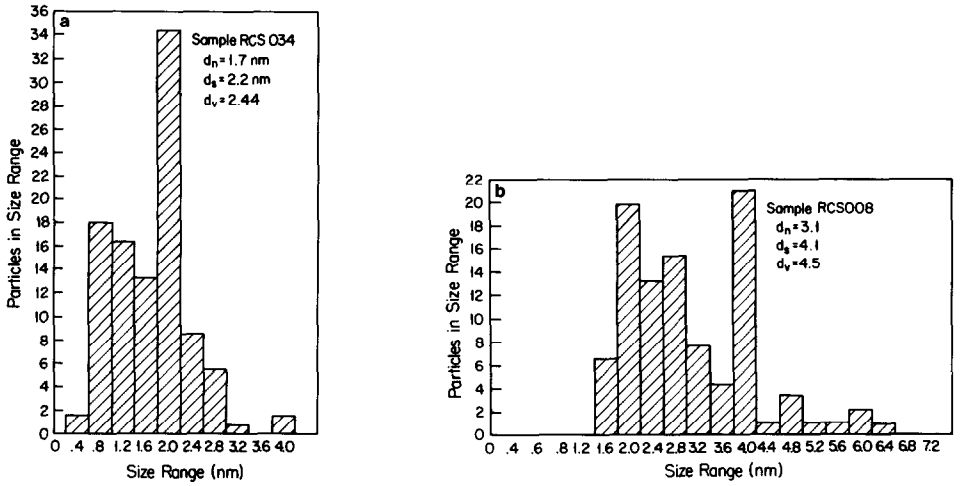

FIG. 2. Particle size distributions of bimetallic Ru–Cu/SiO_2 catalysts as determined from TEM images. (a) Catalyst RCS034, (b) catalyst RCS008.

between chemisorption and microscopy results supports the hypothesis that small particles of Ru are decorated by finely dispersed Cu leading to a disruption of the Ru ensembles required for H_2 dissociation.

Individual metal particles in the bimetallic Ru–Cu series catalysts were analyzed by energy dispersive X-ray spectroscopy (EDS). Representative EDS spectra for each catalyst are given in Fig. 3. Thirty particles from different regions of each catalyst sample were analyzed. Based on the relative intensity of Ru and Cu signals, the EDS spectra were grouped into five categories: I, Ru only; II, Ru + Cu, predominant Ru signal; III, Cu + Ru, predominant Cu signal; IV, Ru + Cu, approximately equal Ru and Cu signal; V, Cu only. This qualitative classification is similar to the one used previously in the case of Ru–Au catalysts (*17, 18*) and allows an approximate determination of the composition of bimetallic particles by signal averaging and scaling factor correction. Scaling factors for X-ray intensities were normalized with respect to the intensity of the K lines of Si. For the semiquantitative compositional analysis of individual metal particles in supported Ru–Cu catalysts, the Ru L lines with a scaling factor of 1.81, and Cu K lines with a scaling factor of 1.73 were used. Implicit assumptions in the approach to the semiquantitative analysis of small metal particles are the applicability of the thin foil criterion and the absence of fluorescence effects (*38, 39*). A reliable quantitative analysis of the composition of individual small metal particles is not possible in view of the poor X-ray counting statistics. Attempts to improve the X-ray counting statistics by extending the counting time were generally unsuccessful due to severe problems with beam damage upon prolonged exposure of a small sample area to the electron beam. Grouping of EDS spectra of similar appearance into five categories provided some improvement of the signal-to-noise ratio and resulted in useful semiquantitative information on typical particle compositions. The percentage of particles falling into each spectral category are summarized in Table 3. Particles larger than 4 nm were generally monometallic Cu, and bimetallic cluster formation was confined to a size range of 1.5 to 4 nm. Particles smaller than 1.5 nm gave only Ru signals. For such small particles, of course, no individual particle analysis was possible due to the extremely low X-ray count. The electron beam had to be rastered over a small region containing numerous such

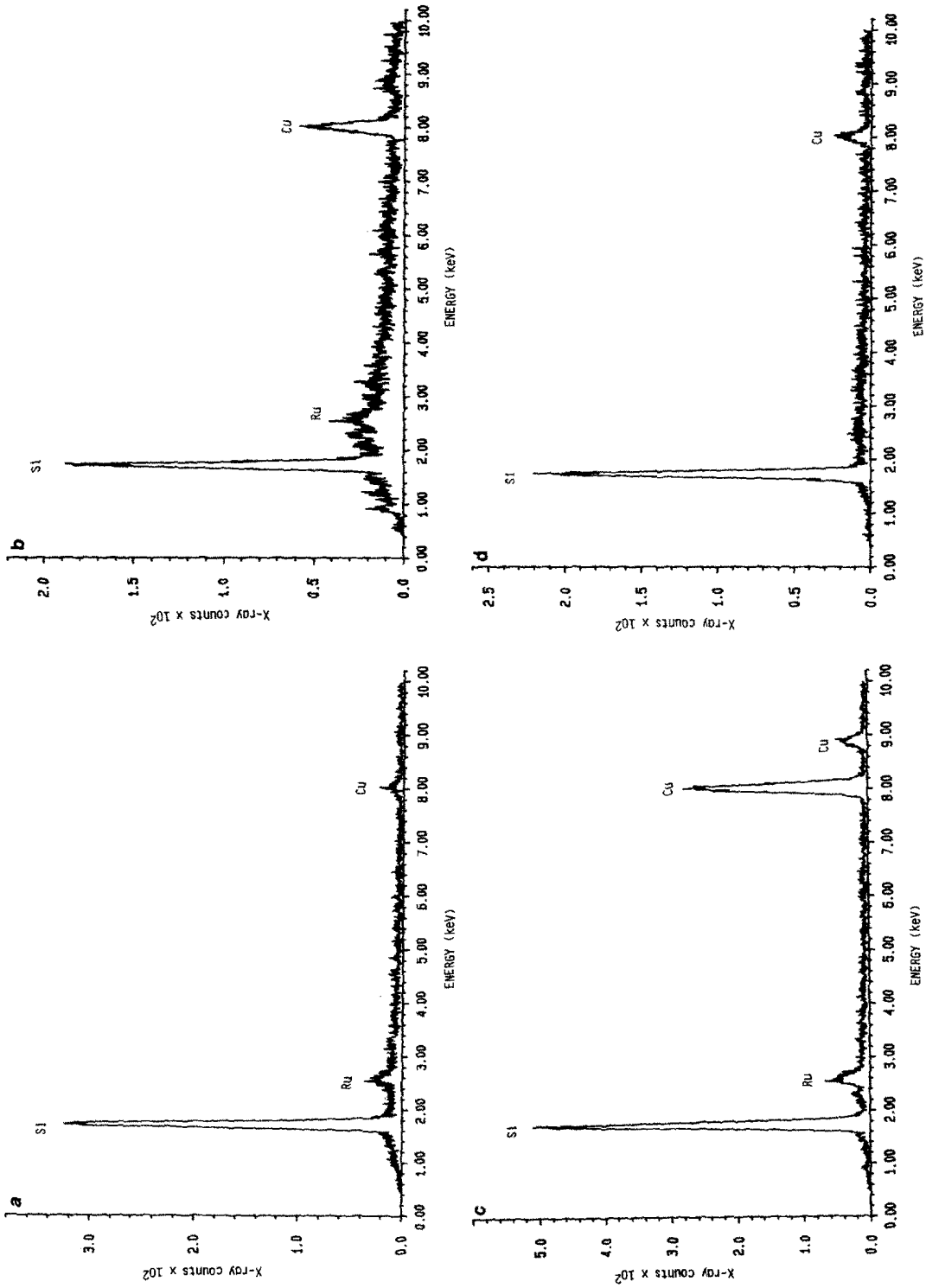

FIG. 3. Typical EDS spectra obtained from individual metal particles in Ru–Cu/SiO_2 catalysts: (a) 3-nm particle in catalyst RCS034 (spectral category IV), (b) another 3-nm particle in catalyst RCS034 (spectral category III), (c) 4-nm particle in catalyst RCS008 (spectral category III), (d) 5-nm particle in catalyst RCS008 (spectral category V).

TABLE 3

EDS Spectral Categories for Bimetallic Samples

Sample code	Percentage of particles in each category				
	I Ru only	II Ru + Cu (trace)	III Ru trace + Cu	IV Ru + Cu (1 : 1)	V Cu only
RCS034	16.67	8.33	25.0	50.0	0
RCS008	0	0	67.0	0	33

small metal particles to get a measurable X-ray signal. In catalyst RCS034, approximately 4/5 of the particles were bimetallic, giving both Ru and Cu signals. However, the relative intensity of Ru and Cu signals varied from particle to particle, giving rise to spectra falling into spectral categories II, III, and IV. More than half of the bimetallic particles appeared to contain approximately equal amounts of Ru and Cu. In catalyst RCS008, metal particles larger than 4 nm were without exception monometallic Cu, while the smaller particles were Cu rich bimetallic clusters. On such nonuniform bimetallic catalysts, it appears to be very difficult to derive information on the ensemble size requirements for catalytic reactions in view of the heterogeneity in particle composition (even for very small clusters). The particle composition does not appear to be a function of particle shape.

Microdiffraction experiments were carried out to gain a better understanding of the structure of small bimetallic clusters. We were limited to a probe size of 10 nm with the LaB_6 gun used in the JEOL-100CX microscope. In view of the small size of these bimetallic clusters, the use of a field emission gun with a probe size of 1 nm would have been desirable. Despite the instrumental limitations, diffraction patterns from individual metal particles could be ob-

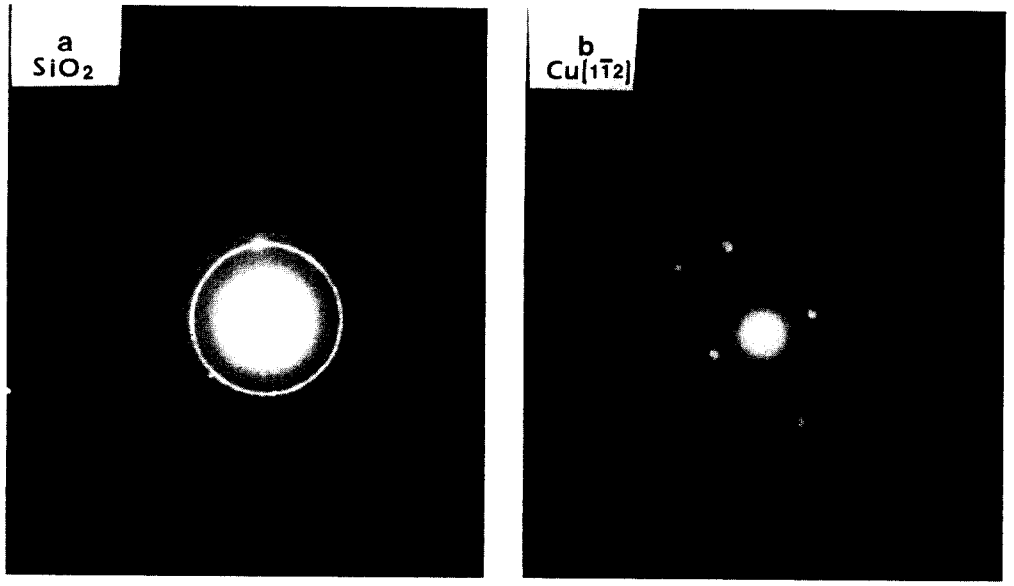

FIG. 4. Microdiffraction patterns. (a) Typical ring pattern of SiO_2 support, (b) [112] zone axis diffraction pattern obtained from a 4-nm Cu-rich particle in catalyst RCS008.

tained provided that the particle of interest was the only metal particle within a 10-nm diameter, thin specimen region. Figure 4 shows some of the electron diffraction patterns. Most of the diffraction spots obtained from small metal particles could be ascribed to either Ru or Cu, confirming that the Ru–Cu bimetallic clusters are either Ru particles decorated by Cu or Cu particles decorated by Ru. These observations are in qualitative agreement with the hypothesis regarding the structure of bimetallic clusters advanced by Sinfelt *et al.* (*1–3*).

CONCLUSIONS

A study of Ru–Cu/SiO_2 catalysts was undertaken with special emphasis on characterization by chemisorption and analytical electron microscopy. Bimetallic clusters were identified in the size range 1.5 to 4 nm. Particles larger than 4 nm were, without exception, monometallic Cu. Microdiffraction spots could be assigned to Ru or Cu only, suggesting no significant structural modification of the two metal components. Our results are in agreement with Sinfelt's concept of "bimetallic clusters" where one metal component is chemisorbed on the other. Considerable heterogeneity in composition was observed from one particle to the next. This makes it rather difficult to derive any information on the ensemble sizes required for a particular reaction from measurements of catalytic activities on these supported bimetallic Ru–Cu catalysts.

In our catalysts, the chemisorption of H_2 was found to be significantly suppressed by the presence of Cu. Cu seems to inhibit the H_2 dissociation capability of Ru by disrupting the required Ru ensembles. A minimum of six adjacent Ru sites seems to be necessary for dissociative H_2 chemisorption (*11, 13*). The amount of strongly bound H_2 decreases and the reversible uptake of H_2 increases (expressed as percentage of total gas uptake) as more and more Cu is dispersed on the Ru surface. Attempts to carry out H_2/O_2 titration in order to distinguish between Ru and Cu surface sites proved to be unsuccessful. So far, no suitable temperature regime could be found where O_2 adsorbed on one metal component was completely titratable by H_2 with reasonable equilibration times. On our bimetallic samples, spillover of H_2 to Cu sites did not play a major role due to the suppression of H_2 dissociation by Cu, resulting in a small concentration of atomic hydrogen. Comparing small bimetallic Ru–Cu and Ru–Au particles supported on SiO_2 (*23*), it appears that the relative interdispersion of Ru and the Group Ib metal must be different since the ensemble size requirements for H_2 dissociation are violated in the case of Ru–Cu but not for Ru–Au. In the Ru–Au system, the majority of the EDS spectra consisted of predominantly Ru or Au signals with a trace signal of the other component. In the Ru–Cu catalysts, a large fraction of the EDS spectra shows signals of both elements with approximately equal intensity.

Conflicting reports in the literature on supported Ru–Cu bimetallic catalysts (*1–9*) and Cu-covered Ru(0001) single crystal surfaces (*10–16*) are probably due to different sample preparation conditions used by various research groups leading to variations in the relative Ru and Cu interdispersion. For example, we find in agreement with Sinfelt *et al.* (*1*) that the impregnation of SiO_2 with $Cu(NO_3)_2$ alone leads to the formation of comparatively large Cu particles, whereas coimpregnation of the SiO_2 support with $RuCl_3$ and $Cu(NO_3)_2$ solution leads to the formation of small bimetallic particles. Obviously, more research is necessary to understand the role of preparative variables on the final characteristics of supported or single crystal samples. This and structural identification of small bimetallic clusters are subjects of current research in our laboratory.

ACKNOWLEDGMENTS

Financial support of this work through the National Science Foundation and by the Army Research Office

is gratefully acknowledged. The authors would like to thank Dr. Giorgio R. Tauszik for participating in catalyst preparation and characterization.

REFERENCES

1. Sinfelt, J. H., *J. Catal.* **29,** 308 (1973).
2. Sinfelt, J. H., Lam, Y. L., Cusumano, J. A., and Barnett, A. E., *J. Catal.* **42,** 227 (1976).
3. Sinfelt, J. H., *Acc. Chem. Res.* **10,** 15 (1977).
4. Prestridge, E. B., Via, G. H., and Sinfelt, J. H., *J. Catal.* **50,** 115 (1977).
5. Helms, C. R., and Sinfelt, J. H., *Surf. Sci.* **72,** 229 (1978).
6. Bond, G. C., and Turnham, B. D., *J. Catal.* **45,** 128 (1976).
7. Lai, S. Y., and Vickerman, J. C., *J. Catal.* **90,** 337 (1984).
8. Rouco, A. J., Haller, G. L., Oliver, J. A., and Kemball, C., *J. Catal.* **84,** 297 (1983).
9. Haller, G. L., Resasco, D. E., and Wang, J., *J. Catal.* **84,** 477 (1983).
10. Christmann, K., Ertl, G., and Shimizu, H., *J. Catal.* **61,** 397 (1980).
11. Shimizu, H., Christmann, K., and Ertl, G., *J. Catal.* **61,** 412 (1980).
12. Vickerman, J. C., Christmann, K., and Ertl, G., *J. Catal.* **71,** 175 (1981).
13. Vickerman, J. C., and Christmann, K., *Surf. Sci.* **120,** 1 (1982).
14. Peden, C. H. F., and Goodman, D. W., *in* "Proceedings, Symposium on the Surface Science of Catalysis, Philadelphia, Aug. 1984," ACS Symposium Series.
15. Yates, J. T., Jr., Peden, C. H. F., and Goodman, D. W., *J. Catal.* **94,** 576 (1985).
16. Goodman, D. W., and Peden, C. H. F., *J. Catal.* **95,** 321 (1985).
17. Datye, A. K., and Schwank, J., *in* "Proceedings, 8th International Congress on Catalysis, Berlin," Vol. IV, p. 587. Verlag Chemie, Weinheim, 1984.
18. Datye, A. K., and Schwank, J., *J. Catal.* **93,** 256 (1985).
19. Datye, A. K., Lee, J. Y., Shastri, A. G., and Schwank, J., AIChE Annual Meeting, 1984, San Francisco, Calif., Paper No. 53a.
20. Tauszik, G. R., Leofanti, G., and Galvagno, S., *J. Mol. Catal.* **25,** 357 (1984).
21. Bassi, I. W., Garbassi, F., Vlaic, G., Marzi, A., Tauszik, G. R., Cocco, G., Galvagno, S., and Parravano, G., *J. Catal.* **64,** 405 (1980).
22. Galvagno, S., Schwank, J., Parravano, G., Garbassi, F., Marzi, A., and Tauszik, G. R., *J. Catal.* **69,** 283 (1981).
23. Shastri, A. G., and Schwank, J., *J. Catal.* **95,** 271 (1985).
24. Shastri, A. G., and Schwank, J., *J. Catal.* **95,** 284 (1985).
25. Shastri, A. G., and Schwank, J., *J. Catal.* **98,** 191 (1986).
26. Galvagno, S., Schwank, J., and Parrravano, G., *J. Catal.* **61,** 223 (1980).
27. Sinfelt, J. H., Via, G. M., and Lytle, F. W., *J. Chem. Phys.* **72,** 4832 (1980); *J. Chem. Phys.* **67,** 3831 (1977).
28. Allard, L. F., and Blake, D. F., *in* "Microbeam Analysis—1982" (K. F. J. Heinrich, Ed.), p. 8. San Francisco Press, California.
29. Goldstein, J. I., Costley, J. L., Lorimer, G. W., and Reed, S. J. B., *in* "Scanning Electron Microscopy" (O. Johari, Ed.), Vol. I, p. 315, 1977.
30. Dubois, A. H., *Surf. Sci.* **119,** 399 (1982).
31. Boerio, F. J., and Armogan, L., *Appl. Spectrosc.* **32,** 509 (1978).
32. Ali, S., and Wood, G. C., *Corrosion Sci.* **8,** 413 (1968).
33. Lawless, K. R., and Gwathmey, A. T., *Acta Metall.* **4,** 153 (1956).
34. Shi, S. K., Lee, H. I., and White, J. M., *Surf. Sci.* **102,** 56 (1981).
35. Anderson, J. R., "Structure of Metallic Catalysts." Academic Press, New York, 1975.
36. Yang, C.-H., and Goodwin, J. G., Jr., *J. Catal.* **78,** 182 (1982).
37. King, T. S., Iwaniya, J. H., Walker, R. D., Goretzke, W. J., and Gerstein, B. C., AIChE 1985 Annual Meeting, Chicago, Ill., November 1985, Paper No. 45a.
38. Williams, D. B., "Practical Electron Microscopy in Materials Science." Electron Optics Publishing Group, New Jersey, 1984.
39. Goldstein, J. I., Hren, J. J., and Joy, D. C., "Introduction to Analytical Electron Microscopy." Plenum, New York, 1979.